Korean J. Chem. Eng., **31**(10), 1892-1897 (2014)
DOI: 10.1007/s11814-014-0145-9

pISSN: 0256-1115
eISSN: 1975-7220

Electrical and optical characteristics of Ar plasma generated by low-frequency (60 Hz) power source

Hong Tak Kim, Chang-Duk Kim, Myoung Sik Pyo, and Chinho Park†

School of Chemical Engineering, Yeungnam University, Gyeonsan 712-749, Korea
(*Received 1 October 2013 • accepted 22 May 2014*)

Abstract−The optical and electrical properties of Ar plasma, ignited using low-frequency (LF, 60 Hz) power source, were investigated. The plasma resistance, electron temperature, and density were found to be $\sim 10^2\ \Omega$, ~3 eV and $\sim 10^8$ cm^{-3}, respectively. The plasma parameters are strongly dependent on Ar pressure and discharge current, and the results of optical emission analysis showed similar tendency to the probe measurements. The properties of Ar plasma are similar to DC-pulsed discharge, and the polarity of AC power can be possible of depositions and modifications on both conductive and insulating materials, unlike DC discharge. The a-C films, which are deposited using Ar-diluted CH_4 plasma, showed a smooth surface, high transmittance (>80%), high sp^3 concentration (~40%) and wide optical band-gap (3.55 eV). Consequently, the LF power source was found to be a very simple, convenient and inexpensive tool to generate plasmas for various applications.

Keywords: 60 Hz, Amorphous Carbon, Argon, Low-frequency, Plasma Parameter

INTRODUCTION

Plasma is used as a materials processing tool to allow various film depositions and surface modifications at lower temperatures. The energy of particles involved in the plasma processing is relatively high compared to those in chemical and thermal processing, and also there exist various radicals to make chemical reactions to proceed more rapidly [1-4]. This means that the temperature of chemical and physical processes can be reduced dramatically, leading to the synthesis and modification of materials at lower temperatures. Thus, plasma processing has been applied to many industrial fields such as semiconductor and display device fabrications, protective coatings, and decorative coatings [1-6]. Generally, the processing plasma is generated by DC and high frequency power sources in RF (13.56 MHz) or microwave (2.45 GHz) frequencies. However, the plasma using low-frequency (LF, 60 Hz) power source is not frequently applied to the materials processing such as film deposition and surface modification, although this frequency is the conventional AC power frequency in many countries. One of the reasons for not using LF frequency is that the plasma, generated using LF power source, does not typically generate continuous discharges contrary to DC and RF discharges. However, the molecular plasma using LF power source has relatively high electron temperature compared to that of DC or RF plasmas [7,8]. The reason for this is the reduction of energy loss for the excitation of molecular bonding and the increased of energy transmittance [7,8]. In addition, the LF power source is readily available and inexpensive, and it does not require the matching network system needed for high frequency power source or the rectification system needed for DC power source. Kim et al. recently applied the molecular plasma for deposition of metal and insulator films using LF power source and reported that these plasmas can be useful for film depositions [5,6]. However, there are few results for applications using Ar atomic plasma generated by LF-power, and the properties of the plasma have not been investigated in detail.

In this study, Ar plasma was generated using LF power source, and the effects of pressure and discharge current were investigated on plasma parameters using optical and electrical measurements. In addition, amorphous carbon films were deposited on glass substrate using Ar plasma by adding a small quantity of methane (CH_4) gas and the properties of the films were studied.

EXPERIMENT DETAILS

The experimental apparatus consisted mainly of three parts: the reaction chamber system, the power system, and the plasma diagnostics system. The plasma discharge chamber was stainless steel with a diameter of 22 cm and a height of 18 cm. The electrodes were also stainless steel with a diameter of 10 cm, and configuration of the electrodes was in a traditional diode type with a gap of 5 cm. The Ar gas was used as discharge gas, and the flow rate was controlled by a mass flow controller. The pressure was monitored using a convector gauge (Varian, EYESYS) and an ion gauge (Kodivac, WNI-1000). The base pressure was 5×10^{-5} Torr, which was obtained by a mechanical pump and a diffusion pump. The plasma was generated using an LF (60 Hz) power source (2,000 V, 1 A). The basic electrical properties of the discharge were investigated with an oscilloscope (Tektronix, TDS3012) and multi-meters (Keithley 2000, Tektronix DM2510G). The optical emission spectra (OES) of the plasma were observed with a photodiode array spectrometer (Ocean Optics S2000). The parameters of the discharge were measured by a single Langmuir probe, in which the probe tip was made of tungsten wire with a diameter 0.25 mm and a length of 4 mm. The Langmuir probe system consisted of a power supply (Keithley HV 248), a chemical

†To whom correspondence should be addressed.
E-mail: chpark@ynu.ac.kr
Copyright by The Korean Institute of Chemical Engineers.

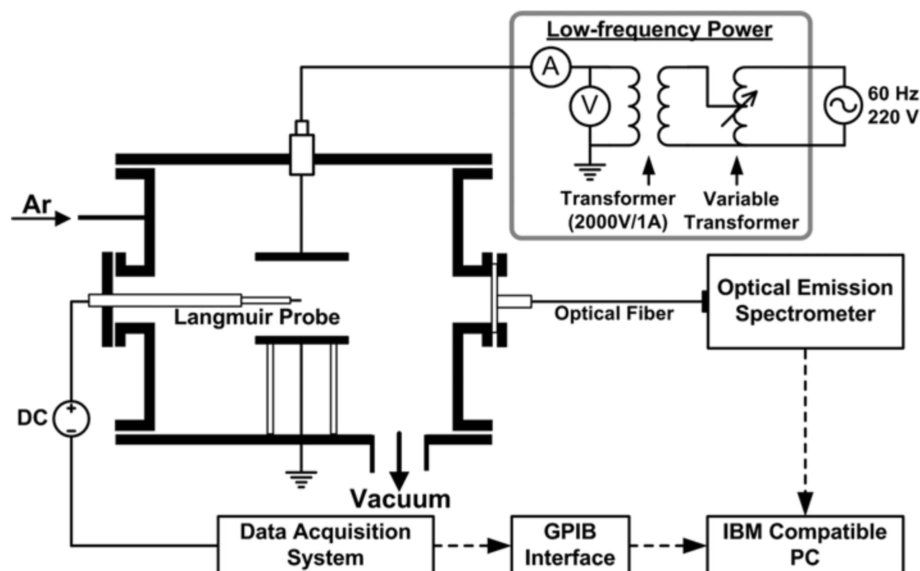

Fig. 1. The schematic diagram of the experimental setup for the diagnostics of Ar plasma generated using low-frequency (60 Hz) power source.

battery, a digital multi-meter (Keithley, 2000), and a single probe. The deposition of carbon films was also performed using Ar-diluted CH_4 plasma. The total pressure was 1 Torr and the ratio of Ar : CH_4 gas was 25 : 1. The applied current was fixed at 120 mA and deposition time was 1 hr. The substrate temperature was kept at room temperature (25 °C) during depositions. The optical properties, vibrational properties, and morphology of the films were measured with UV-Vis spectrometer (Varian, Cary 500G), Raman spectrometer (Horiba, SPEX 1403) and SEM (Hitachi S- 4200), respectively. The schematic diagram of experimental setup for the diagnostics of Ar plasma and the deposition of carbon films is shown in Fig. 1.

RESULTS AND DISCUSSION

The relationship between breakdown voltage and pressure in Ar plasma is shown in Fig. 2. The breakdown voltage abruptly dropped when the pressure was increased from base pressure to 50 mTorr, and then the voltage gradually increased when the pressure increased above 50 mTorr. In the breakdown voltage decreasing region, the mean free path of electrons is much longer than that in higher pressure region, and this means there are few collisions between electrons and other particles [2,5,8]. Thus, the increase of pressure up to 50 mTorr leads to the increase of collision probability, and thus the breakdown voltage rapidly decreases. On the other hand, the breakdown voltage increases in the region of higher pressure (greater than 50 mTorr), and this region should have different mechanisms to ignite discharges compared to the discharge in the lower pressure region. In the region of higher pressure, there are enough collisions between the electrons and other particles, and the energy loss process due to collisions plays an important role to determine the breakdown voltage. The increase of pressure causes the rise of energy loss due to more frequent collisions, and this leads to the increase of the breakdown voltage, which again means the discharge is more difficult [2,5,8,9].

Fig. 3(a) shows the oscillogram of the discharge generated by

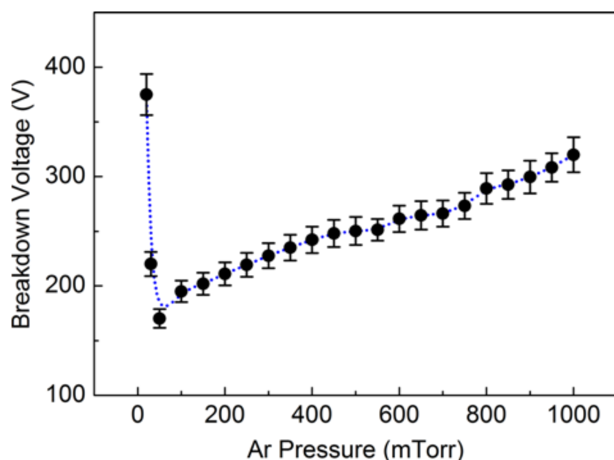

Fig. 2. The breakdown voltage of Ar plasma as a function of Ar pressure.

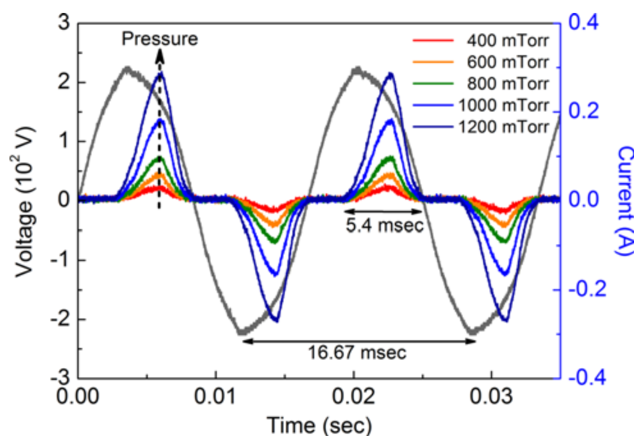

Fig. 3. The oscillogram of current (I(t)) and voltage (V(t)) as a function of time.

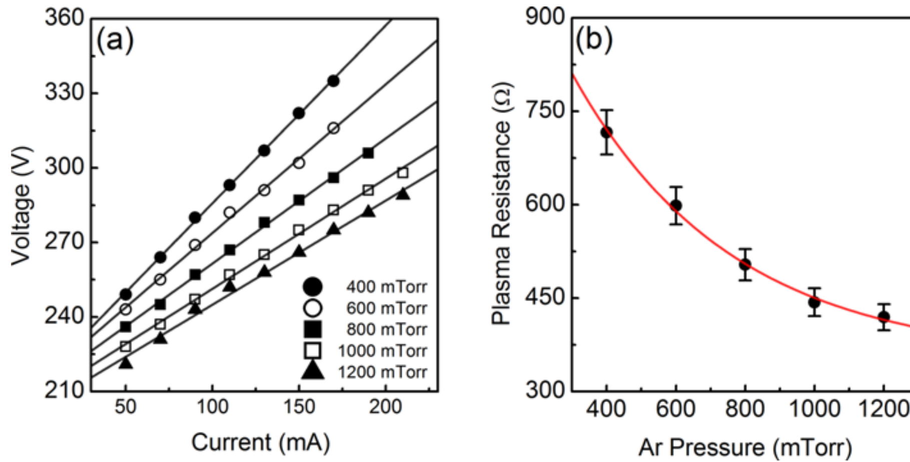

Fig. 4. Electrical properties of Ar plasma generated using a low-frequency power source; (a) voltage-current line at different Ar pressure, and (b) plasma resistance as a function of Ar pressure.

the LF power source. A phase shift between current and voltage was not observed, and this implies the LF plasma has resistive properties. Thus, it is expected that the LF plasma obeys Ohm's law, and this can be verified using the relationship between current and voltage. Fig. 4(a) shows the current to voltage (I-V) curve according to the Ar pressure. The I-V curve nearly exhibits a linear relationship, and the slope of the curves depends strongly on the gas pressure. From these results, we can conclude that the LF plasma is a resistive discharge, and the I-V curve of discharge well obeys Ohm's law. Now, the discharge resistance can be defined as the ratio of the discharge voltage and the discharge current. The discharge resistance gradually decreases with the increase of Ar pressure, and the values of a discharge resistance in the Ar plasma have the order of 10^2 Ω. This can be explained by an increase of the charged particles due to inelastic collisions as well as the decrease of sheath thickness [2,8]. The change of the discharge resistance as a function of the Ar pressure is shown in Fig. 4(b). Fig. 5 shows the electron temperature and density of the Ar plasma at different pressures. The current to voltage (I-V) curve from the Ar plasma was measured using a single probe, and the electron temperature (T_e) and the electron density (n_e) were calculated using Maxwellian distribution. The relationship between the electron current (I_e) on the probe and applied voltage (V) is given by [5,8,10]:

$$I_e(V) = j_{es}A_P \exp\left(-\frac{e(V_P - V)}{kT_e}\right) \quad (1)$$

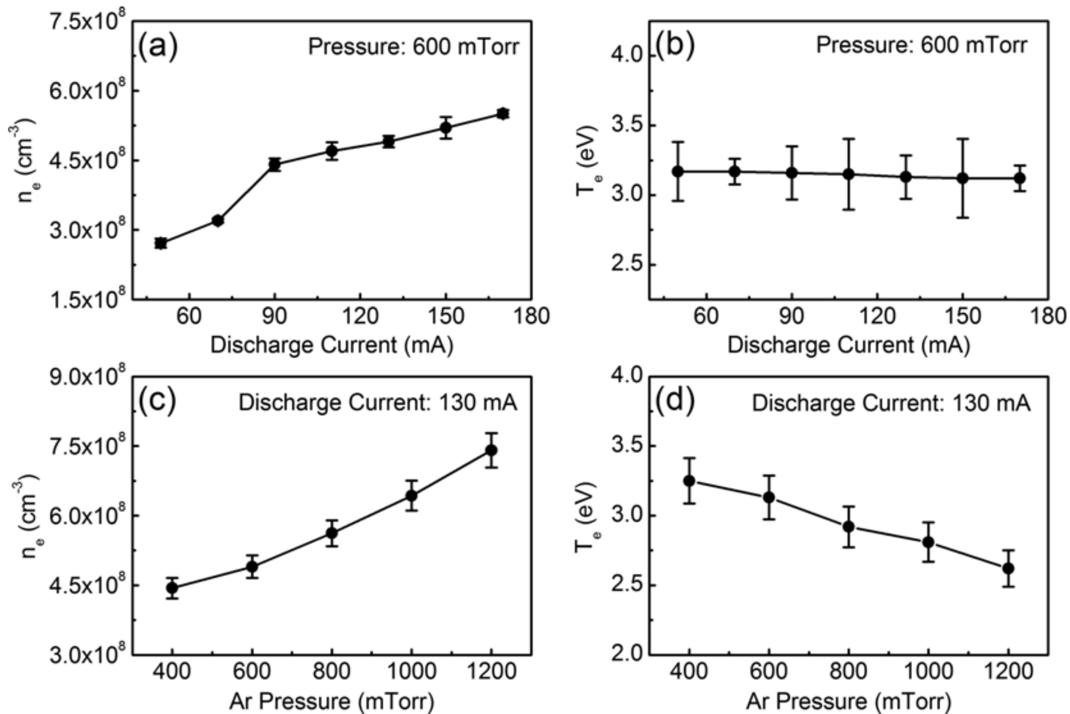

Fig. 5. Plasma parameters at different discharge conditions; (a) n_e and (b) T_e according to discharge current (Ar pressure: 600 mTorr), and (c) n_e and (d) T_e according to Ar pressure (discharge current: 130 mA).

where j_{es} is the electron saturation current density, V_p is the plasma potential, A_p is the effective surface area of the probe, and T_e is the electron temperature. T_e is calculated by taking the natural log for $I_e(V)$ in Eq. (1) and plotting $\ln[I_e(V)]$ with respect to V. The inverse of the slope in the graph of $\ln[I_e(V)]$-V gives the electron temperature of the Ar plasma. Using the values of T_e, A_p, and I_{es}, the electron density n_e is given by [5]:

$$n_e = 3.78\times10^{11}\frac{I_{es}}{A_p T_e^{1/2}} \quad (2)$$

As the discharge current and the Ar pressure increase, the n_e also increases. However, T_e seldom changes with the increasing discharge voltage, and the effect of Ar pressure is predominant in the change of T_e. The calculated n_e ranges from 2.7×10^8 to 8.4×10^8 cm^{-3}, and T_e ranges from 3.25 eV to 2.55 eV at different discharge conditions. Usually, n_e is mainly related to the collision probability between electrons and particles, and T_e is closely associated with the energy from the electric field in the time of collisions [2,3,5,10]. The increase of Ar pressure causes more frequent collisions of electrons with neutral or charged particles. The increase of the collision rate enhances the population of electrons, and also this restricts electrons from acquiring enough energy from the electric field [3,5].

Fig. 6 shows the optical emission spectrum of the Ar plasma generated by the LF power source (Ar pressure: 600 mTorr, discharge current: 130 mA). Mainly observed optical emissions in the Ar discharge were singly-ionized argon lines (Ar II) and unionized argon lines (Ar I) [11,12]. These emission lines originated from the inelastic collisions of electrons with neutral or ionized Ar particles. The emission intensity is proportional to the density of electronically excited species, and also the intensity of Ar II lines reflects the relative population among various energy levels of the Ar ions. Thus, the emission intensity is closely related to the electron density, and the increase of electron impact processes causes the enhancement of emission intensity from the Ar plasma. Fig. 7 shows the change of emission intensity for Ar I and Ar II according to the discharge current and Ar pressure. As the discharge current and Ar pressure increases, the optical emission intensities of Ar I and Ar II also increase with the similar tendency observed in the probe measurements. In

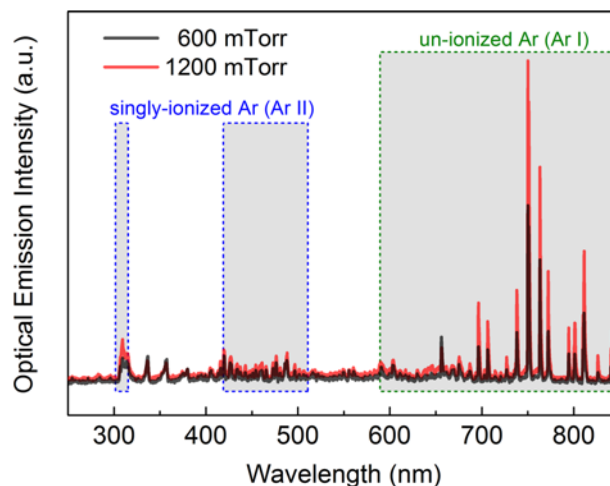

Fig. 6. The optical emission spectrum of Ar plasma using a low-frequency power source (Discharge current: 130 mA).

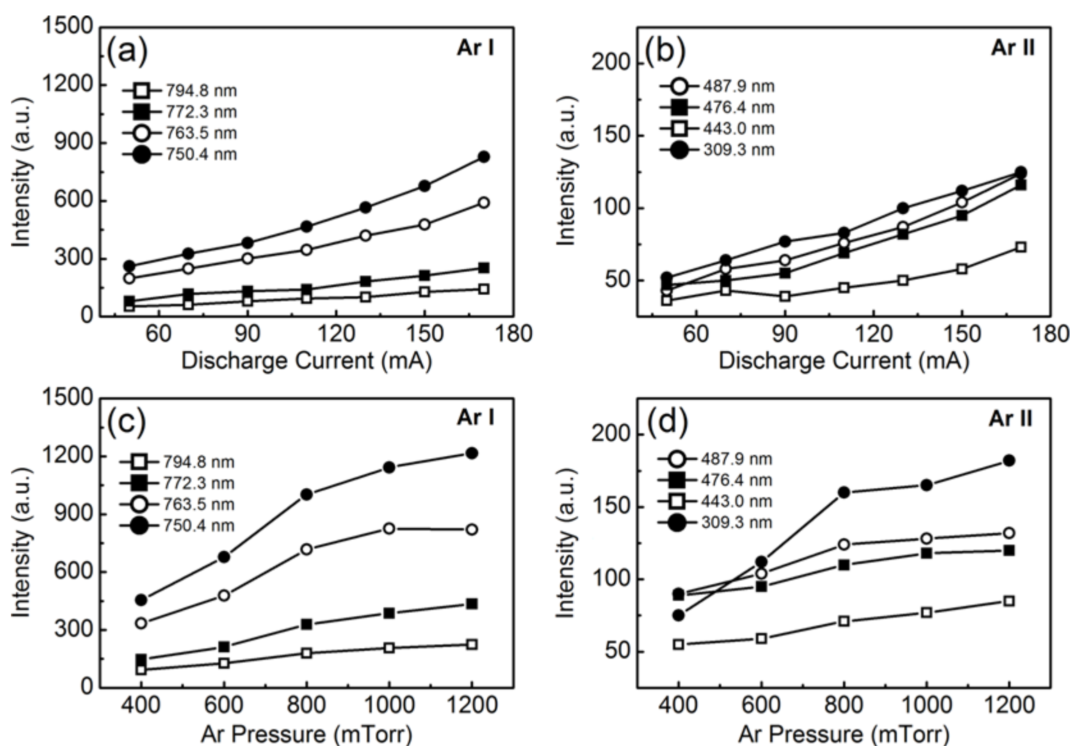

Fig. 7. The variation of optical emission intensity of excited species in Ar plasma; (a) unionized Ar lines (Ar I) and (b) singly-ionized Ar lines Ar (II) according to discharge current (Ar pressure: 600 mTorr), and (c) Ar I and (d) Ar II according to Ar pressure (discharge current: 130 mA).

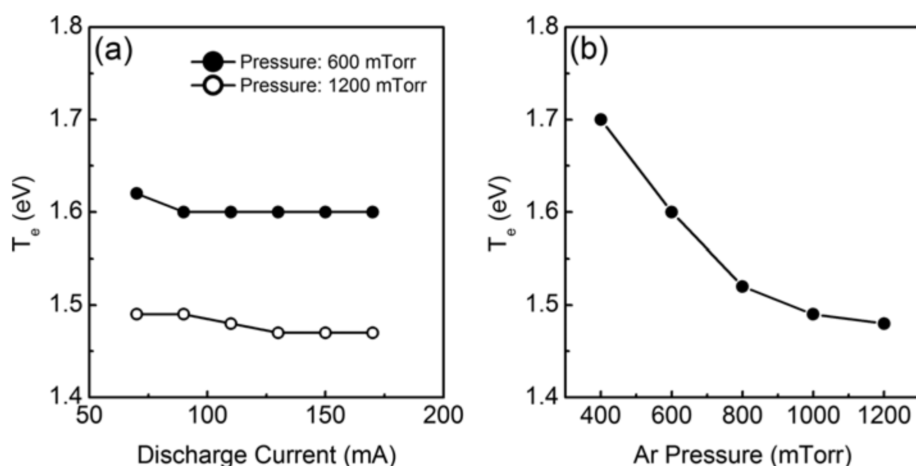

Fig. 8. The electron temperature (T_e) calculated using the relative intensity method; (a) T_e at different discharge current and (b) T_e at different Ar pressure.

addition, the electron temperature can be calculated from the relative intensity method [12] and the equation is given by:

$$\frac{I_{ij}}{I_{kl}} = \frac{\lambda_{kl} A_{ij} g_i}{\lambda_{ij} A_{kl} g_k} \exp\left(-\frac{E_i - E_k}{kT_e}\right) \tag{3}$$

where I_{ij} and I_{kl} are the spectral intensity, λ_{ij} and λ_{kl} are the wavelength, A_{ij} and A_{kl} are the transition probability, g_i and g_k are the statistical weight, E_i and E_j are the excitation energy and k is the Boltzmann constant. This equation is represented the relationship between T_e and the ratio of emission peaks in thermal equilibrium or local thermal equilibrium (LTE) state. Fig. 8 shows the electron temperature using the relative intensity method. The electron temperature values are low compared to the results of probe measurement; however, the tendency is consistent with the probe results. From these results, it is expected that the emission intensity of various Ar I and Ar II lines can be utilized as an indicator to diagnose the plasma conditions.

The a-C films were deposited on glass substrate to verify the effects of Ar plasma. The effects of CH_4 in plasma properties could be ignored because the quantity of CH_4 was too small compared to that of Ar, and the discharge condition for film depositions was chosen at the point of saturated electron density and middle value of electron

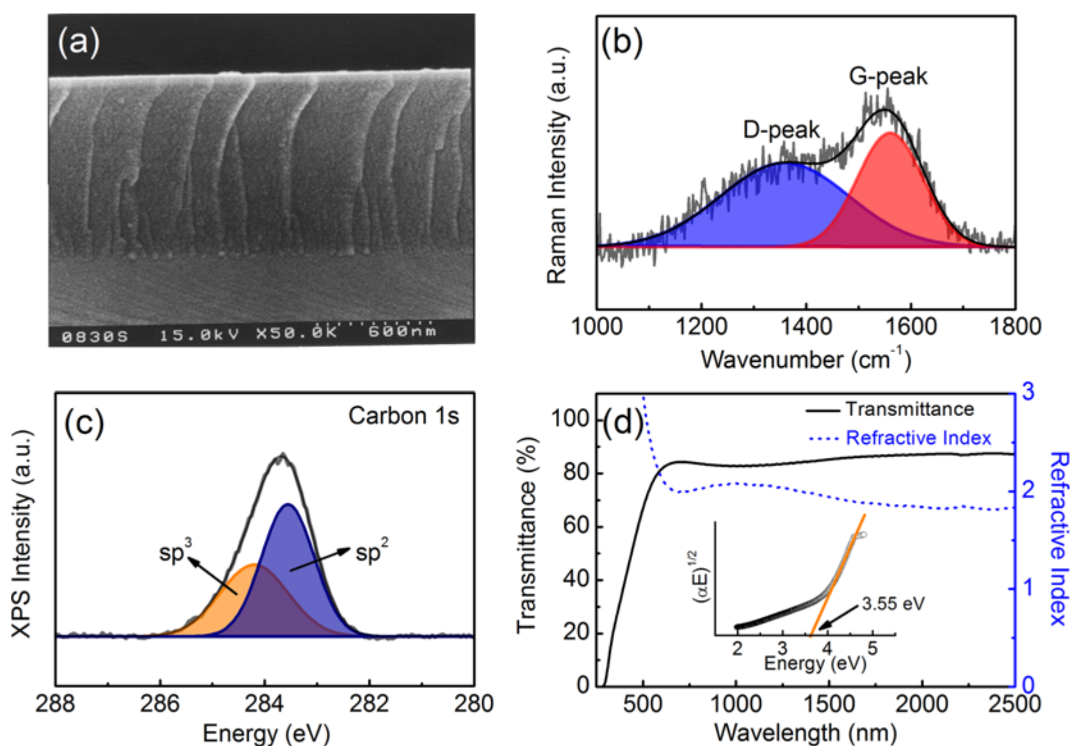

Fig. 9. The properties of a-C films deposited by Ar-diluted CH_4 plasma; (a) cross-sectional SEM image of a-C films, (b) Raman spectrum of a-C films, (c) Gaussian de-convolution of carbon 1s peak in XPS spectrum, (d) transmittance spectrum and refractive index of a-C films.

Table 1. The properties of a-C films deposited by Ar-diluted CH_4 plasma generated using LF power source

Parameter	Unit	Value
Deposition rate	[nm/min]	15
Ratio of sp^2	[%]	60
Ratio of sp^3	[%]	40
Transmittance (@600 nm)	[%]	82
Refractive Index (@600 nm)		2.14
Optical Band-gap	[eV]	3.55

temperature. a-C films consist of a mixture of sp^2 and sp^3 bonding and have interesting properties such as a wide optical band gap, thermal stability, high resistivity, transparency in visible and infrared region, and chemical inertness for both acids and alkali [13-16]. In this study, deposited a-C films represented very smooth surface and a traditional amorphous phase as shown in Fig. 9(a) and 9(b). Usually, a-C films are composed of a mixture of sp^2 and sp^3 bonding and these contents played an important role to determine the properties of films [5,13,14]. The content of sp^2 and sp^3 was evaluated from de-convolution of carbon 1s peak in XPS spectrum and the content of sp^3 bonding in as-deposited a-C films reached up to about 40% as shown in Fig. 9(c). The optical properties of a-C films were calculated from the transmittance spectrum [13] and are shown in Fig. 9(d). The a-C films exhibited high transmittance and wide band-gap property, and it is thought these properties originate from the high ratio of sp^3 in a-C films. Usually, the optical band-gap in a-C films can be defined as the difference between π-π^* state in sp^2 and σ-σ^* state in sp^3 bonding contributes to more higher energy levels [1,2,5]. However, high concentration of sp^3 can increase the influence of σ-state, and it is thought that this makes the band-gap be wide. The properties of a-C films are summarized in Table 1.

CONCLUSIONS

The electrical and optical properties of the Ar plasma, which was generated by a low-frequency power source, were investigated in detail. It was found that the n_e is strongly dependent on both the discharge current and the Ar pressure, but, on the contrary, T_e is only dependent on the Ar pressure. The orders of plasma resistance, n_e, and T_e of the Ar plasma are estimated to be about ~10^2 Ω, ~10^8 cm^{-3} and 2-3 eV, respectively. Furthermore, the variation tendency in the n_e is very similar to the change of optical emission intensity for the Ar I and Ar II lines, which means the optical emission intensity can be applied as an indirect indicator to diagnose the density of Ar plasma. The a-C films which were deposited using Ar-diluted CH_4 plasma, showed a smooth surface, high transmittance (>80%), high sp^3 concentration (~40%) and wide optical band-gap (3.55 eV). Consequently, the Ar plasma, generated by a low-frequency power source, behaves similarly to the plasma generated by the DC-pulsed discharge with a polarity. Thus, this method can be applied to the plasma processes for the deposition of both conductor and dielectric materials unlike DC-discharge. In addition, it is concluded that the plasma processing using a low-frequency power source can be applied to various applications in simple laboratory experiments, because the low-frequency power source is readily available, simple to engage and inexpensive.

ACKNOWLEDGEMENT

This work was supported by the 2012 Yeungnam University research grant (212-A-380-259).

REFERENCES

1. K. K. Schuegraf, *Handbook of thin film deposition processes and techniques: Principles, methods, equipment, and applications*, Noyes Publication, New Jersey (1988).
2. M. A. Lieberman and A. J. Lichtenberg, *Principles of plasma discharges and materials processing*, Wiley, New York (1994).
3. A. Fridman, *Plasma chemistry*, Cambridge University Press, New York (2008).
4. A. W. Adamson and A. P. Gast, *Physical chemistry of surfaces*, Wiley, New York (1997).
5. H. T. Kim and S. H. Sohn, *Vacuum*, **86**, 2146 (2012).
6. H. T. Kim, M. J. Kim and S. H. Sohn, *J. Phys. Chem. Solids*, **73**, 931 (2012).
7. M. Shimozuma, K. Kitamore, H. Ohno, H. Hasegawa and H. Tagashira, *J. Electron. Mater.*, **14**, 573 (1985).
8. H. T. Kim, D. K. Park and W. S. Choi, *J. Korean Phys. Soc.*, **42**, S916 (2003).
9. B. Chapman, *Glow discharge processes: Sputtering and plasma etching*, Wiley, New York (1980).
10. D. N. Ruzic, *Electrical probes for low temperature plasmas*, AVS Press, New York (1994).
11. National Institute of Standards and Technology (NIST) *Atomic spectra database data*, http://www.nist.gov/atomic-spectroscopy.cfm.
12. H. R. Griem, *Principle of plasma spectroscopy*, Cambridge University Press, Cambridge, UK (1997).
13. J. Robertson, *Mater. Sci. Eng.*, **R37**, 129 (2002).
14. J. Robertson, *Surf. Coat. Technol.*, **50**, 185 (1992).
15. M. W. Geis and M. A. Tamor, *Encyclopedia of applied physics*, VCH Publishers, New York (1993).
16. J. Mort and F. Jansen, *Plasma deposited thin films*, CRC Press, Boca Raton (1986).